

Laser & Optoelectronics Progress

C-Band 53.76 Tbit/s Transmission Based on Bit Allocation Optimization with Raman Amplification

Ding Junjie¹, Wang Chen¹, Ju Zhou¹, Zhu Bowen¹, Sang Bohan¹, Liu Bo², Yu Jianjun^{1*}

¹Key Laboratory for Information Science of Electromagnetic Waves (MoE), Fudan University, Shanghai 200433, China;

²Nanjing University of Information Science and Technology, Nanjing 210044, Jiangsu, China

Abstract We experimentally demonstrate an 80-channel wavelength division multiplexing (WDM) transmission system over a 400 km fiber link. Raman amplification results in a non-flat WDM signal spectrum. Therefore, bit allocation optimization is used to enable different channels to carry different order quadrature amplitude modulation signals according to their optical signal-noise-ratios. A neural network equalizer based on a convolutional neural network (CNN), long short-term memory (LSTM) network, and fully connected (FC) layer structure is adopted in Rx digital signal processing, in which CNN is used for characteristic extraction, LSTM is used for equalization and demodulation, and FC layers are used for output. After transmission, the bit error rate of all channels is below the 25% soft-decision forward error correction threshold, and the line rate reaches 53.76 Tbit/s.

Key words wavelength division multiplexing transmission; Raman amplification; bit allocation optimization; neural network equalizer

中图分类号 TN929.1 文献标志码 A

DOI: 10.3788/LOP223344

1 Introduction

Improving spectral efficiency via high-order quadrature amplitude modulation (QAM) formats for high-capacity transmission has been extensively investigated in coherent wavelength division multiplexing (WDM) transmission systems^[1-7]. Stimulated Raman scattering (SRS) results in power transfer from short-wavelength channels to long-wavelength channels, which changes the signal power distribution across wavelengths along fiber propagation. The application of distributed Raman amplification (DRA) and, in general, the dependence of amplified spontaneous emission (ASE) noise on the wavelength results in a wavelength-dependent optical signal-noise-ratio (OSNR), where a longer wavelength channel has a larger OSNR. Therefore, a wavelength-dependent method is required to prevent the introduction of large system margins. Power allocation has become the method of choice to limit the imbalance caused by Raman amplification^[8-15]. However, power optimization based on the analytical Gaussian noise

(GN) model has high calculation complexity and limits the exploitation of the WDM system capacity to the maximum^[16-20].

In this study, we propose an optimization method based on bit allocation that produces a higher exploitable capacity while being straightforward to implement. In the bit allocation optimization method, the QAM format per wavelength channel is identified using the received OSNR. Compared with power optimization based on a mathematical model, bit allocation optimization has very low complexity and does not require detailed knowledge of the characteristics of the network components, especially the parameters of the fiber and optical amplifier. For the first time, we designed a hybrid convolution neural network, long short-term memory network, and fully connected layer (CNN-LSTM-FC) structure for polarization division multiplexing (PDM) QAM signal equalization while incorporating a combination of the advantages attributed to the CNN, LSTM network, and FC layer structure^[21-28]. In a C-band coherent WDM system covering a 4 THz bandwidth, we experimentally

收稿日期: 2022-12-19; 修回日期: 2023-01-19; 录用日期: 2023-02-22; 网络首发日期: 2023-03-02

基金项目: 国家重点研发计划(2018YFB1800900)、国家自然科学基金(61935005, 61720106015, 61835002, 62127802)

通信作者: *jianjun@fudan.edu.cn

demonstrated an 80-channel 50 GHz grid transmission employing 48 Gbaud PDM QAM signals using a bit allocation method. Owing to the neural network (NN) equalizer, 53.76 Tbit/s WDM transmission over 400 km standard single mode fiber (SSMF) has been achieved, satisfying the 25% soft-decision forward error correction (SD-FEC) threshold.

2 Experimental setup

The experimental setup is shown in Fig. 1. Tx digital signal processing (DSP) comprises a pre-equalization and raised-cosine (RC) filter with 0.01 roll-off factor. Eighty WDM channels were produced at the transmitter, consisting of odd-channel (Ch. 1, 3, 5, \dots , 79) and even-channel (Ch. 2, 4, 6, \dots , 80) groups. We used 80 external cavity lasers (ECLs) with less than 100 kHz linewidth to generate WDM channels operating from 1531.51 nm to 1563.05 nm. The 40 channels in the odd-channel group corresponded to the H18-57 channels in the ITU-T standard with a 100 GHz frequency spacing, while the 40 channels in the even-channel group corresponded to the C18-57 ITU-T channels with a 100 GHz frequency spacing. Furthermore, two polarization-maintaining arrayed waveguide gratings (PM-AWG) were used to combine the odd and even channels.

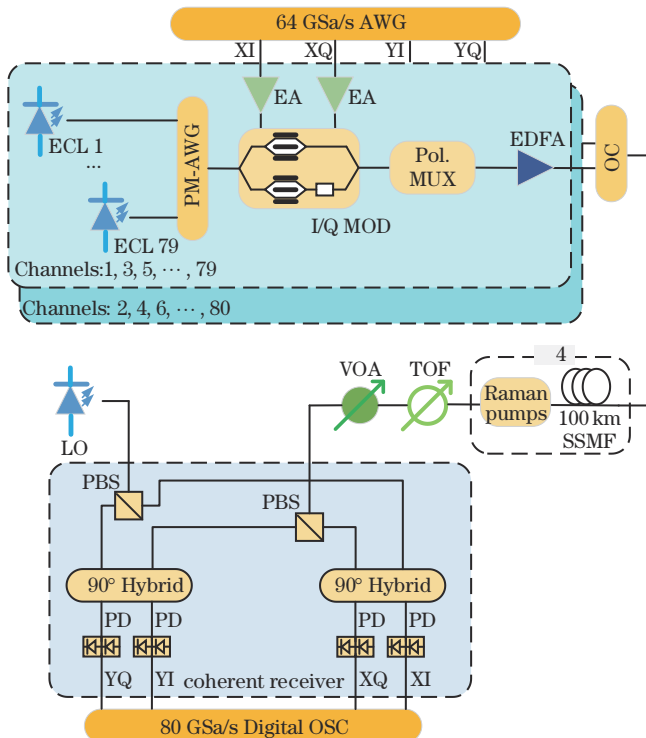


Fig. 1 Experimental setup of 80-channel coherent WDM transmission

The output electrical signals from the four independent channels (I_{odd} , Q_{odd} , I_{even} , and Q_{even}) of a 64 Gsa/s sampling rate arbitrary waveform generator (AWG) were boosted and fed into two 30 GHz in-phase/quadrature (I/Q) modulators in the odd-channel and even-channel groups. After the I/Q modulator, a polarization multiplexer comprising a 3 dB polarization-maintaining optical coupler (PM-OC), 1 m PM optical delay line, and polarization beam combiner (PBC) was used to generate PDM optical signals. Subsequently, an erbium-doped fiber amplifier (EDFA) was added to adjust the launch optical power into the fiber link. The fiber link consisted of four spans of 100 km SSMF with an attenuation coefficient of 0.188 dB/km. Each span had an ~ 18 dB ON-OFF gain backward-pumped Raman amplifier. Fig. 2 shows photographs of the experimental setup comprising 80 ECLs and a 4×100 km fiber link with Raman amplifiers.

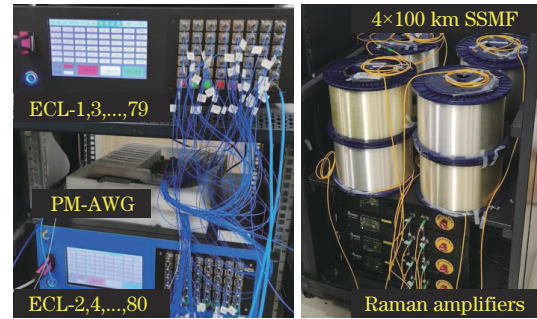


Fig. 2 Photographs of the experimental setup comprising 80 ECLs and a 4×100 km fiber link with Raman amplifiers

The optical spectra of WDM signals employing the 256QAM format before and after fiber transmission at 0.02 nm resolution are illustrated in Fig. 3 (a) and (b), respectively. SRS results in a non-flat optical spectrum after Raman amplification. The OSNR in a short-wavelength channel is low, and, unlike a long-wavelength channel, a short-wavelength channel cannot support high-order QAM formats. Therefore, to approach the maximum capacity of the WDM system, we adopted the bit allocation optimization method, where different channels carry QAM signals of different orders according to their OSNR.

After the fiber transmission, a tunable optical filter (TOF) was used to select the received optical signal of each test WDM channel. In addition, a variable optical attenuator (VOA) was added to adjust the input optical power into an integrated coherent receiver. We used another ECL signal as an optical local oscillator (LO) for homodyne detection. After optical-to-electrical conversion, the received PDM signals were captured

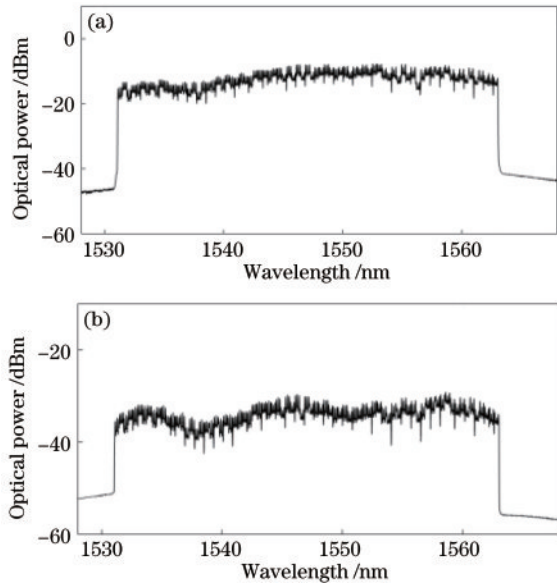


Fig. 3 Spectra. (a) WDM signals fiber launch spectrum; (b) output spectrum after fiber transmission with Raman amplification

by an 80 GSa/s sampling rate oscilloscope with a 36 GHz electrical bandwidth. In the offline Rx-side DSP, an NN equalizer based on the CNN-LSTM-FC structure was used after resampling, chromatic dispersion (CD) compensation, constant-modulus algorithm (CMA) equalization, frequency offset, and carrier phase estimation.

3 NN structure

In the NN equalizer, we designed a hybrid CNN-LSTM-FC structure, as illustrated in Fig. 4. The front CNN layers extract high-order features of the input data, which compresses the input data [29]. The reported LSTM-FC layer structure has been widely verified to be effective in NN equalizers [30]. The proposed hybrid CNN-LSTM-FC layer structure combines the advantages

of various NN layers. Therefore, the effectiveness of the NN equalizer is significantly higher than that of an NN equalizer consisting of single-type layers [31]. Because the PDM QAM signals can be depicted by four real data points: I_x , Q_x , I_y , and Q_y , the input dimension of the network is $T \times 4$, where T represents the memory depth of the network. After the input block, there are four cascaded one-dimensional convolution (1D Conv) layers in the CNN block. For simplicity, the parameters of the four 1D convolutional layers are the same. The tap of the convolution kernel was set to 1×7 to achieve its optimal performance. The number of feature maps constructed by the convolution layer was set to 24 to balance the performance and calculation complexity. The values of the convolution kernels were initialized using Gaussian weight initialization. The activation function of the CNN block was the ReLU function. At the end of the CNN block, a max-pooling layer was used to reduce the number of calculation parameters and eliminate information redundancy. The LSTM layer is a common model used in NN equalizers owing to its capability for storing time-domain information of the input. The hidden units of the two LSTM layers were set to 128 and 64. Subsequently, two fully connected layers, which contained 50 and 20 neural units, were used to output the I_x , Q_x , I_y , and Q_y values of the PDM-QAM signals. The nonlinear activation function of these two fully connected layers was a sigmoid function suitable for the output of the LSTM layer. A dropout layer was set after the first FC layer to suppress overfitting of the neural network. The loss function of the entire network was set as the mean squared error function. The batch size and training epochs were set to 64 and 40, respectively. The gradient optimizer was adapted from Adam.

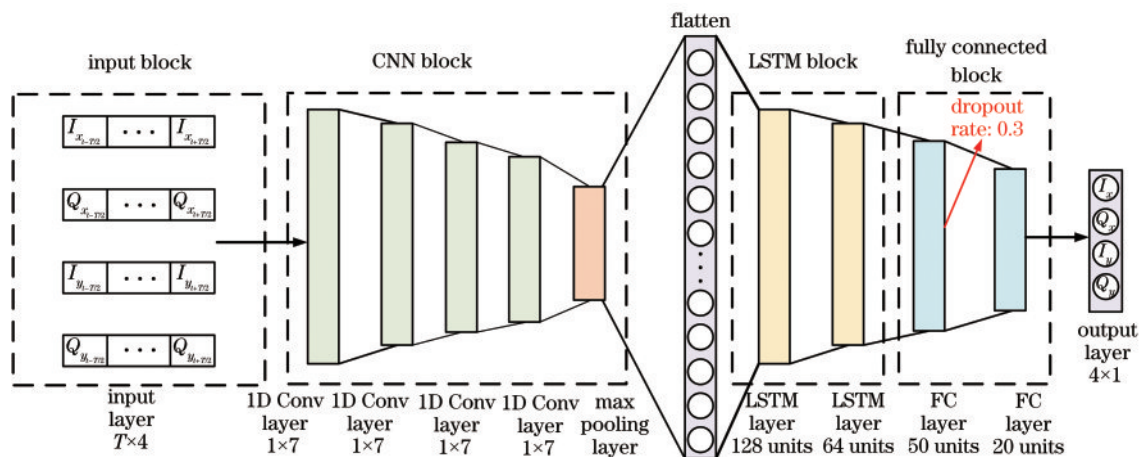


Fig. 4 Schematic overview of NN equalizer based on CNN-LSTM-FC structure

4 Results and discussions

First, we loaded the same data into the AWG in the transmitter and selected the optical signal of each wavelength channel using the TOF in the receiver. An optical spectrum analyzer was used to capture the selected optical signal and measure its OSNR. The received OSNR after fiber transmission versus the wavelength is shown in Fig. 5. Subsequently, in the bit allocation optimization method, the QAM format per wavelength channel was identified by the received OSNR. Therein, 26 long-wavelength channels (1552.93–1563.05 nm) carried 256QAM signals, 26 short-wavelength channels (1531.51–1541.35 nm) carried 64QAM signals, and the remaining 28 channels of the intermediate wavelength (1541.75–1552.52 nm) carried 128QAM signals. For each wavelength channel, we loaded the data with the corresponding QAM format into the AWG in the transmitter and selected the signal of this channel via the TOF in the receiver. The total line rate of this WDM transmission system was $(26 \times 6 + 28 \times 7 + 26 \times 8) \times 2 \times 48 = 53.76$ Tbit/s.

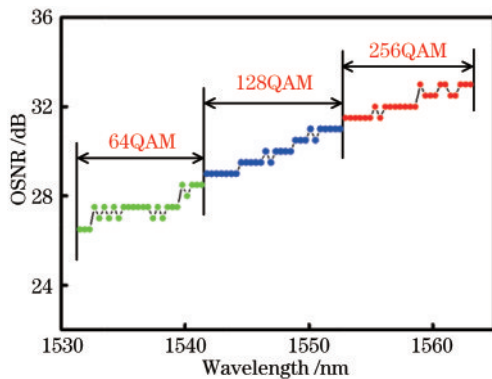


Fig. 5 Received OSNR versus wavelength

As shown in Fig. 6, after 400 km fiber transmission, the bit error rate (BER) of each channel

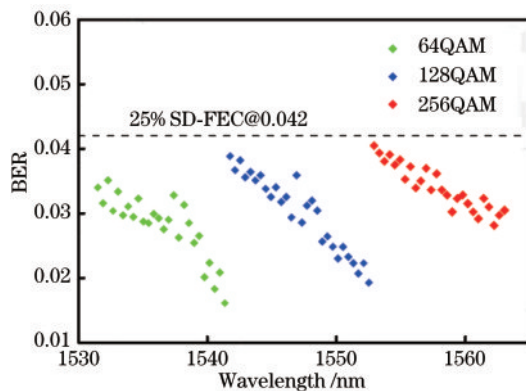


Fig. 6 BER of all 80 channels after fiber transmission

is below the 25% SD-FEC threshold at 4.2×10^{-2} . Considering a 25% SD-FEC overhead, the net bit rate is thus $53.76 \times 0.8 = 43.008$ Tbit/s.

5 Conclusions

An 80-channel 50 GHz grid WDM transmission employing 48 Gbaud PDM signals was demonstrated using the bit allocation optimization method. Owing to the NN equalizer based on a hybrid CNN-LSTM-FC structure, 53.76 Tbit/s line rate (43.008 Tbit/s net rate) transmission over a 400 km fiber link can be achieved.

References

- [1] Kobayashi T, Shimizu S, Nakamura M, et al. 13.4-Tb/s WDM transmission over 1, 280 km repeated only with PPLN-based optical parametric inline amplifier[C]//2021 European Conference on Optical Communication (ECOC), September 13-16, 2021, Bordeaux, France. New York: IEEE Press, 2021.
- [2] Kato T, Watanabe S, Yamauchi T, et al. Whole band wavelength conversion for wideband transmission[C]//2021 Optical Fiber Communications Conference and Exhibition (OFC), June 6-10, 2021, San Francisco, CA, USA. New York: IEEE Press, 2021.
- [3] Cai J X, Mazurczyk M V, Vedala G, et al. 9 Tb/s transmission using 29 mW optical pump power per EDFA with 1.24 Tb/s/W power efficiency over 15, 050 km[C]//Optical Fiber Communication Conference (OFC) 2021, June 6-11, 2021, Washington, DC. Washington, D. C.: Optica Publishing Group, 2021: Th4C.5.
- [4] Ding J J, Sang B H, Wang Y Y, et al. High spectral efficiency WDM transmission based on hybrid probabilistically and geometrically shaped 256QAM[J]. Journal of Lightwave Technology, 2021, 39(17): 5494-5501.
- [5] Wang L, Gao M Y, Zhang Y L, et al. Optical phase conjugation with complex-valued deep neural network for WDM 64-QAM coherent optical systems[J]. IEEE Photonics Journal, 2021, 13(5): 7200308.
- [6] Xu J, Qiu Y, Deng N. Optical phase remodulation for Rayleigh noise mitigation in 10 Gb/s/channel WDM passive optical networks[J]. Chinese Optics Letters, 2017, 15(6): 060604.
- [7] Yu S H, Luo M, Li X, et al. Recent progress in an 'ultra-high speed, ultra-large capacity, ultra-long distance' optical transmission system (Invited Paper)[J]. Chinese Optics Letters, 2016, 14(12): 120003-120007.
- [8] Kobayashi T, Morimoto M, Ogoshi H, et al. PDM-16QAM WDM transmission with 2nd-order forward-pumped distributed Raman amplification utilizing incoherent pumping[C]//2019 Optical Fiber Communications Conference and Exhibition (OFC), March 3-7, 2019, San Diego, CA, USA. New York: IEEE Press, 2019.
- [9] Ionescu M, Renaudier J, Ghazisaeidi A, et al.

- Optimization of power efficient spatial division multiplexed submarine cables using adaptive transponders and machine learning[J]. *Journal of Lightwave Technology*, 2022, 40(6): 1597-1604.
- [10] Puttnam B J, Luis R S, Rademacher G, et al. S, C and extended L-band transmission with doped fiber and distributed Raman amplification[C]//2021 Optical Fiber Communications Conference and Exhibition (OFC), June 6-10, 2021, San Francisco, CA, USA. New York: IEEE Press, 2021.
- [11] Tan M M, Iqbal M A, Krzaczanowicz L, et al. Optimization of Raman amplification schemes for single-span high data rate coherent transmission systems[C]//2021 Conference on Lasers and Electro-Optics (CLEO), May 9-14, 2021, San Jose, CA, USA. New York: IEEE Press, 2021.
- [12] Bao H H, Jin W, Ho H L. Tuning of group delay with stimulated Raman scattering-induced dispersion in gas-filled optical fiber[J]. *Chinese Optics Letters*, 2020, 18(6): 060601.
- [13] Nishikimi K, Sano A. Pumping scheme for ultra-wideband WDM transmission using distributed Raman amplification[C]//2022 27th OptoElectronics and Communications Conference (OECC) and 2022 International Conference on Photonics in Switching and Computing (PSC), July 3-6, 2022, Toyama, Japan. New York: IEEE Press, 2022.
- [14] Zheng L, Chen Z Y, Wu D M, et al. Channel distributions of the transient power overshoot in backward-pumped Raman amplified WDM systems[J]. *Chinese Optics Letters*, 2004, 2(9): 503-504.
- [15] Xue F, Qiu K, Chen Y. Research on WDM optical fiber transmission system based on fiber Raman amplifier[J]. *Chinese Optics Letters*, 2003, 1(10): 564-566.
- [16] Lasagni C, Serena P, Bononi A. A Raman-aware enhanced GN-model to estimate the modulation format dependence of the SNR tilt in C+L band[C]//45th European Conference on Optical Communication (ECOC 2019), September 22-26, 2019, Dublin, Ireland. London: IET, 2020.
- [17] Ferrari A, Pileri D, Virgillito E, et al. Power control strategies in C+L optical line systems[C]//2019 Optical Fiber Communications Conference and Exhibition (OFC), March 3-7, 2019, San Diego, CA, USA. New York: IEEE Press, 2019.
- [18] Buglia H, Sillekens E, Vasylychenkova A, et al. On the impact of launch power optimization and transceiver noise on the performance of ultra-wideband transmission systems[J]. *Journal of Optical Communications and Networking*, 2022, 14(5): B11-B21.
- [19] Bononi A, Antona J C, Serena P, et al. Pump-constrained capacity maximization: to flatten or not to flatten? [C]//2021 European Conference on Optical Communication (ECOC), September 13-16, 2021, Bordeaux, France. New York: IEEE Press, 2021.
- [20] Lasagni C, Serena P, Bononi A, et al. Power allocation optimization in the presence of stimulated Raman scattering[C]//2021 European Conference on Optical Communication (ECOC), September 13-16, 2021, Bordeaux, France. New York: IEEE Press, 2021.
- [21] Häger C, Pfister H D. Nonlinear interference mitigation via deep neural networks[C]//Optical Fiber Communication Conference, March 11-15, 2018, San Diego, California. Washington, D.C.: Optica Publishing Group, 2018: W3A.4.
- [22] Wu H J, Chen J P, Liu X R, et al. One-dimensional CNN-based intelligent recognition of vibrations in pipeline monitoring with DAS[J]. *Journal of Lightwave Technology*, 2019, 37(17): 4359-4366.
- [23] Chen M A, Jin X Q, Li S B, et al. Compensation of turbulence-induced wavefront aberration with convolutional neural networks for FSO systems[J]. *Chinese Optics Letters*, 2021, 19(11): 110601.
- [24] Liu J W, Wang Y J, Yang H F, et al. Transfer learning aided PT-CNN in coherent optical communication systems[C]//2022 20th International Conference on Optical Communications and Networks (ICOON), August 12-15, 2022, Shenzhen, China. New York: IEEE Press, 2022.
- [25] Xu S F, Zou W W. Optical tensor core architecture for neural network training based on dual-layer waveguide topology and homodyne detection[J]. *Chinese Optics Letters*, 2021, 19(8): 082501.
- [26] Zhang H T, Zhang L, Jiang Y, et al. LSTM and ResNets deep learning aided end-to-end intelligent communication systems[C]//2021 2nd Information Communication Technologies Conference (ICTC), May 7-9, 2021, Nanjing, China. New York: IEEE Press, 2021: 156-160.
- [27] Zhang M, Xu B, Li X Y, et al. Traffic estimation based on long short-term memory neural network for mobile front-haul with XG-PON[J]. *Chinese Optics Letters*, 2019, 17(7): 070603.
- [28] Kong M, Sang B H, Wang C, et al. 645-gbit/s/carrier PS-16QAM WDM coherent transmission over 6, 800 km using modified LSTM nonlinear equalizer[C]//2021 European Conference on Optical Communication (ECOC), September 13-16, 2021, Bordeaux, France. New York: IEEE Press, 2021.
- [29] Wang C, Wang K H, Tan Y X, et al. High-speed terahertz band radio-over-fiber system using hybrid time-frequency domain equalization[J]. *IEEE Photonics Technology Letters*, 2022, 34(11): 559-562.
- [30] Sang B H, Zhou W, Tan Y X, et al. Low complexity neural network equalization based on multi-symbol output technique for 200+ Gbps IM/DD short reach optical system[J]. *Journal of Lightwave Technology*, 2022, 40(9): 2890-2900.
- [31] Freire P J, Osadchuk Y, Spinnler B, et al. Performance versus complexity study of neural network equalizers in coherent optical systems[J]. *Journal of Lightwave Technology*, 2021, 39(19): 6085-6096.